EPR, ENDOR, CD, and MCD Spectra of [^{63}Cu]Cobalamin[1]

Kenneth A. Rubinson*

Contribution from the University Chemical Laboratory, Cambridge CB2 1EW, England.
Received August 11, 1978

Abstract: The circular dichroism (CD), magnetic circular dichroism (MCD), and frozen solution electron paramagnetic resonance (EPR) and electron nuclear double resonance (ENDOR) spectra are reported for copper cobalamin, the copper-containing analogue of vitamin B_{12}. The ligand is extracted from *Chromatium vinosum*. g value, ^{63}Cu hyperfine splitting, and ^{14}N superhyperfine splitting parameters are evaluated. The metal bonding scheme, with special reference to the separate roles of σ and π bonding, are derived from the spectroscopic parameters. The cobalamin is compared with porphyrin as a ligand.

Vitamin B_{12} and the B_{12} coenzymes are fascinating and biologically ubiquitous coordination complexes and as such have been the subject of many studies of their structure, bonding, and reactions both as coenzymes in their apoproteins[2] and on their own under decidedly nonbiological conditions.[3] To probe the metal chemistry at the cobalt atom, the usual chemical tools used have been changes in axial ligation and changes in cobalt oxidation states.

As a result of these limitations, the interaction between the corrin ring and the metal has been one based mostly on theoretical investigations, since the spectroscopic data in general yield only data about metal-π* interactions. Also, because of significant differences between the naturally occurring corrins and model corrin chromophores containing nickel (e.g., see ref 4), comparisons using the different metals have not been fruitful.

Koppenhagen and Pfiffner showed in a seminal series of papers[5] that metals other than cobalt could be chelated in a natural, metal-free corrin, which was first isolated by Toohey.[6] We report here the spectroscopic characterization of [^{63}Cu]-cobalamin and discuss the insight it gives to the metal-corrin interaction, especially as a probe of the σ bonding.

Experimental Section

Chromatium vinosum strain D was obtained from the Microbiological Research Establishment (Porton Down, Wilts., England). The bacteria were grown[7] on the medium described by Arnon et al.,[8] but with 22 mg/L of 5,6-dimethylbenzimidazole added. The base is incorporated into approximately 90% of the corrins forming hydrogenocobalamin. The cells were received after having been washed, centrifuged, and frozen. Until used, they were stored at −15 °C without any apparent degradation.

The extraction was carried out using a slightly modified procedure of J. J. Pfiffner (personal communication) outlined below. The procedure described is for 450–500 g of the wet cell paste. The entire procedure is carried out in a dark room with red-light illumination using flashlights as needed.

Great care must be taken to eliminate any copper in the reagents used. The water is doubly distilled from glass. Ethanol is glass distilled. Analar acetic acid is twice purified by crystallization. HCl is Aristar grade (BDH, Poole, England). No metal-containing cleaning agents can be used on the glassware.

Frozen cell paste (200–250 g) along with 500 mL of 95% ethanol, 2 mL of acetic acid, and one piece of 18.5-cm Whatman No. 3 filter paper as a filter aid are placed in a blender and mixed for 4–5 min. The mixture is then filtered and the effluent collected. The solid is again mixed 4–5 min with 500 mL of ethanol and the second extract filtered. The total effluent (~2 L from 500 g of cells) is placed in a homemade solvent extractor thermostated at 40 °C and capable of removing 600 mL of ethanol/h. When the total volume is reduced to about 800 mL, water is added equal in milliliters to half the weight of cells in grams. Shortly afterward, *schlieren* are seen in the solvent collector. After that point, 200 mL more solvent is removed. The extracted liquid is acidified to pH 3.5 with HCl (~1 mL of 5 N HCl/50 g of cells). The acidified extract is then centrifuged at 10000g for 15 min at 0 °C, and the liquid decanted. The solid is resuspended and washed with 500 mL of water, the pH brought to 3.5 again, the mixture centrifuged, and the liquid decanted. The collected decanted liquid is neutralized carefully to pH 5.5–6 with solid $NaHCO_3$; this equilibrium is only slowly established. The solution is then degassed under vacuum, an equal volume of water added, and the solution is applied to a washed (3 N HCl in 95% ethanol, then exhaustively water rinsed) column of Amberlite XAD-2 (20–50 mesh, 2.5 × 50 cm) over about 8 h.[9] The loaded column is washed for 10 h with 600 mL of degassed 3 vol % *tert*-butyl alcohol in water. The hydrogenocorrinoids are then eluted with degassed 20 vol % *tert*-butyl alcohol in water, and the effluent is freeze-dried. The quantitation is done spectrophotometrically in aqueous solution using $\epsilon_{490} = 12.5 \times 10^3$ L/(mol·cm).[5a] Typical yields are 0.7–0.8 mg/100 g of cells.

^{63}Cu was purchased (Electromagnetic Separation Group, A.E.R.E., Harwell, Berks., U.K.) as the metal, 99.88% isotopically pure. This was dissolved in hot nitric acid, dried, and dissolved in water to a known concentration. To insert the metal, an excess was added to the cobalamin in an aqueous solution deoxygenated by bubbling with nitrogen. This solution was heated to 60 °C for a few minutes. Completion of the reaction is seen by disappearance of the characteristic red fluorescence. The solution was passed through a small XAD-2 column (0.8 × 3 cm, 100–150 mesh) and the column washed with water and then 4% *tert*-butyl alcohol in water. This removes the impurities having a yellow-green fluorescence. The [^{63}Cu]corrins were eluted off the column using 30 vol % *tert*-butyl alcohol–1% acetic acid in water. The nonfluorescent eluant is then lyophilized. No further purification is necessary since the benzimidazole does not bind the copper, and the differences in side chains on a fraction of the material are not expected to affect the experimental results.

EPR spectra at ambient and liquid nitrogen temperatures were obtained on a significantly modified Varian V-4500 spectrometer with the magnetic field detected with a purpose-built field monitor.[10] Helium temperature EPR and ENDOR spectra were obtained at the ESR Service Center, Medical College of Wisconsin, Milwaukee. The EPR instrument there is a Varian E109 Century Series, and the ENDOR system a Varian E1700 system. With 4 mg of corrin, the ENDOR spectrum was not obtainable at 16 K but only at 4.7 K.

Copper cobalamin doped into polycrystalline vitamin B_{12} was made by rapid (overnight) evaporation of a concentrated B_{12} solution in water with an appropriate amount of the copper compound. EPR line-shape fitting was done first on spectra with unresolved nitrogen splittings. This was done using two different computer simulation programs—one by Dr. P. D. W. Boyd and another from Professor B. Hoffman. The variable values needed for a best fit were in agreement. Both simulation programs calculate g values to second order and include anisotropic line widths. The spectrum is effectively axial. No quadrupole values were needed to have the peaks and zero values of the derivative spectrum fit within 2 G. The nitrogen superhyperfine splittings were determined as discussed in the EPR Results section.

Circular dichroism (CD) and magnetic circular dichroism (MCD) spectra were recorded using a copper cobalamin sample in water at ambient temperature at the laboratory of Dr. A. J. Thomson. The MCD spectra were run two times, with the field in opposite directions. The spectrum shown was calculated from the difference in the two. Calibration of the cobalamin concentration was done using the absorption spectrum with $\epsilon_{490} = 8.33 \times 10^3$ L/(mol·cm).[5b] $[\theta]_M = 3300\Delta\epsilon$ was used to calculate the molar ellipticity.

*Address correspondence to the author at: 1002 Eastwood Rd., Glencoe, Ill. 60022.

0002-7863/79/1501-6105$01.00/0

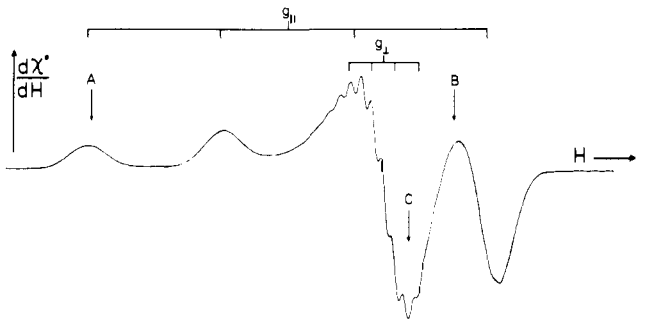

Figure 1. EPR spectrum of a frozen aqueous solution of mixed [^{63}Cu]-corrins: 16.4 K; modulation 10 G, 9.164 GHz. The lettered arrows are the positions of the ENDOR spectra with the same letters shown in Figure 4. The hyperfine line marks are for ^{63}Cu as calculated in the simulation of a spectrum with the superhyperfine structure not showing. The simulation fit was such that on the scale of a published figure, no difference between the experimental and calculated spectra could be seen except for slight deviations in the tails at both ends. Values of the variables used are in Table I.

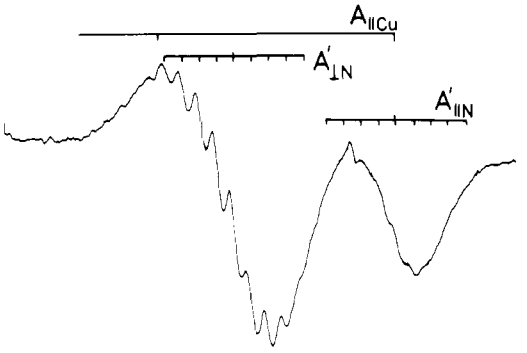

Figure 2. EPR of [^{63}Cu]corrin doped into vitamin B_{12}. The spectrum was obtained at 18 °C. The ^{14}N superhyperfine splitting's line positions shown are in the copper (primed) axis system. Power and modulation levels were such that they did not influence the line shape. Values of the hyperfine constants are given in Table I.

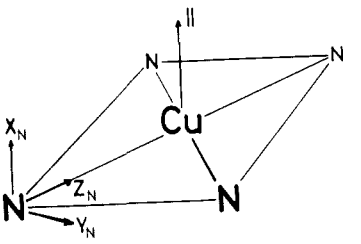

Figure 3. Illustration of the axis system used for the Cu-N_4 chromophore. The analysis described in the text has the nitrogen x and y axes equivalent.

Table I

	TPP[a]	PHTH[b]	corrin[c]
$g_{\parallel}$	2.190	2.160	2.139 (4)
$g_{\perp}$	2.045	2.045	2.037 (2)
$A_{\parallel}$	615		647 (9)
$A_{\perp}$	102.6		105 (6)
A_{iso}	273		286 (7)
A_{aniso}[d]	−342		−361
$A_{\parallel N}$	54.5		48.0 (10)
$A_{\perp N}$	44.1		45.5 (10)
A_{isoN}	47.6		46 (1)
$\Delta_1(xy)$,[e] cm^{-1}	35 400	41 800 (300)	48 600
$\Delta_2(xz,yz)$,[e] cm^{-1}	38 900	38 000 (900)	47 800

[a] All hyperfine values are in MHz. To convert to cm^{-1} × 10^{-4} divide the values in MHz by 3.00. TPP values are from ref 13 and references therein. [b] P. W. Lau and W. C. Lin, *J. Inorg. Nucl. Chem.*, **37**, 2389–2398 (1975). [c] This work. The values in parentheses are the errors in the last digit. The errors for the parameters associated with copper are the values when an obvious misfit occurs in the simulation. For the nitrogen parameters, the errors are estimates from the combined EPR (±0.6 MHz) and ENDOR (±0.5 MHz) spectra. [d] Principal axis. [e] Splitting from the $d_{x^2-y^2}$ orbital calculated using eq 2. The errors for phthalocyanine are from the range in the literature (see footnote *b*).

Results

EPR. Field positions of the principal g values and hyperfine lines determined by the computer simulations using axial symmetry are shown in Figure 1 with the parameter values displayed in Table I. The ^{14}N superhyperfine splitting energies shown have been determined from both the EPR and ENDOR spectra as discussed following. The line positions are shown in Figure 2.

We note that splittings which are experimentally seen and described in gauss in the copper coordinate system, i.e., written $A'_{\perp N}$ and $A'_{\parallel N}$, differ from those expressed in the nitrogen axis system, $A_{\perp N}$ and $A_{\parallel N}$. While gauss or millitesla are the units used to measure splittings, they are unsatisfactory for describing the superhyperfine values in the nitrogen axis system because hyperfine splittings "sensed through" both $g_{\perp}$ and $g_{\parallel}$ contribute to the value of $A_{\parallel N}$ (see eq 1). This relation was originally noted by Guzy and co-workers.[11] With further confusion resulting from having numerous commonly used units (gauss, reciprocal centimeters, tesla, megahertz), much of the past literature on porphyrins and phthalocyanines is unreliable for comparison purposes.[12]

$$A_{\perp N} = A'_{\parallel N} \quad (1a)$$

$$A_{\parallel N} = 2A'_{\perp N} - A'_{\parallel N} \quad (1b)$$

The usual procedure for determining nitrogen superhyperfine interaction constants for copper compounds seems to be to measure the splittings of the peaks of the superhyperfine lines. A more correct method could be to measure the splittings of the midpoints of the lines, since they might more closely reflect the positions of the peaks in the integrated spectrum. However, when we plotted the field values against line number for the peaks seen in Figure 2, the $A'_{\perp N}$ values determined were significantly different depending on the part of the narrow line used. Specifically, the values were 16.5_5, 16.2, and 17.2 G using the peak tops, the midpoints, and the inflection bottoms, respectively. This variation is well outside desired limits, and so a computer simulation program was written that includes anisotropic superhyperfine interactions but with isotropic line widths (M. Manning, personal communication). These simulations suggest that the spectrum in the region shown in Figure 2 results from unresolved $A'_{\perp}$ components with narrow (6–8 G, fwhh) $A'_{\perp N}$ turning points superimposed on them. The variation in $A'_{\perp N}$ values may arise from superhyperfine line-width anisotropy. We choose the best value of $A'_{\perp N}$ = 16.4 (2) G, that is, between the values found from the peak tops and midpoints with the error encompassing both values. Thus knowing the value of $A_{\perp N}$ from the ENDOR spectra (vide infra) and $A'_{\perp N}$ from the EPR, using eq 1b, we find the value of $A_{\parallel N}$. These values are listed in Table I.

ENDOR. Frozen glass electron nuclear double resonance (ENDOR) spectra are capable of obtaining single-crystal-like ENDOR spectra from randomly oriented powders or glasses.[14] Such spectra were obtained to measure the ^{14}N hyperfine splittings, the accuracies of which are at the limits of the powder EPR. The ENDOR spectra obtained at points A, B, and C in Figure 1 are shown in Figure 4. Spectrum A and apparently B (by comparison with A) primarily samples the hyperfine interaction, which is perpendicular to the corrin plane. Spectrum C is primarily sampling the orientations in

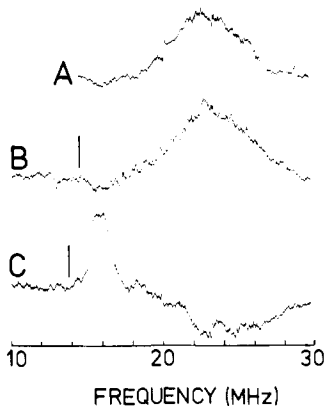

Figure 4. ENDOR spectra recorded at field positions A, B, and C in Figure 1. These are 2740, 3300, and 3255 G, respectively, at 9.165 GHz: modulation amplitude, 40 G; temperature, 4.7 K; power, 8 mW; gain 2, 1.6, 1.6 K, respectively. The peak position and error limits were found by drawing a smooth curve through the spectrum.

the plane of the corrin ring. The spectra seen are from ^{14}N resonances.

The hyperfine structure observed in A is along the nitrogen x axis (Figure 3), that is, $A_{\perp N}$, since we assume axial nitrogen hyperfine symmetry. We expect these spectra to have ENDOR resonances at:[15]

$$\nu_N = \frac{A_{\perp N}}{2} \pm Q \pm Z$$

where Q is the quadrupole coupling constant and Z the nuclear Zeeman term. Z at the magnetic fields used is approximately 1 MHz = 0.333×10^{-4} cm^{-1}. For equivalent nitrogens we expect to see four lines. If the nitrogens are not equivalent as measured by this spectroscopy, we might expect eight lines from two equivalent sets. It is clear from spectra A and B that we do not resolve the lines. However, the peak of A, the experimentally significant ENDOR spectrum, is at 22.5 ± 0.5 MHz = $A_{\perp N}/2$. The values of the perpendicular superhyperfine splitting, $A_{\perp N}$, determined from the EPR spectrum shown in Figure 2 and the ENDOR spectrum agree within experimental error, but the ENDOR data are more reliable.

Spectrum C is composed of the sum of the resonances from all orientations in the plane of the corrin. For the nitrogens, such a spectrum should have the resonance frequencies given by:[15]

$$\nu_N = \frac{A_{\parallel N}}{2}\cos^2\theta + \frac{A_{\perp N}}{2}\sin^2\theta \pm Q(3\cos^2\theta - 1) \pm Z$$

We expect peaks at the turning points at $A_{\parallel N}/2 \pm 2Q \pm Z$ and $A_{\perp N}/2 \mp Q \pm Z$. But the intensities of these peaks are often quite different, as appears to be the case here with only a single peak at 16 MHz evident. Not observing enough peaks to analyze in the above way, we must rely on the EPR spectrum analysis described earlier to obtain the value of $A_{\parallel N}$.

^1H "matrix ENDOR" is usually observed from protic solvents surrounding a paramagnetic center. They are due mainly to dipolar interaction and are usually seen in solids and glasses if there is a proton within 5 to 6 Å of the unpaired spin and the proton's motion is restricted.[16] We expect these signals to occur at the proton Larmour precession frequency ($=g_n\beta_n H/h$), which is shown by the vertical bars in spectra B and C. Given that any solvent water molecular motion will be severely restricted at 4.7 K, this result suggests that there is no water proton within about 6 Å of the copper. This agrees with the chemical and EPR evidence for lack of axial bonding in the copper corrin. Investigation of molecular models suggests that no steric interference to hydration is to be expected from the cobalamin side chains.

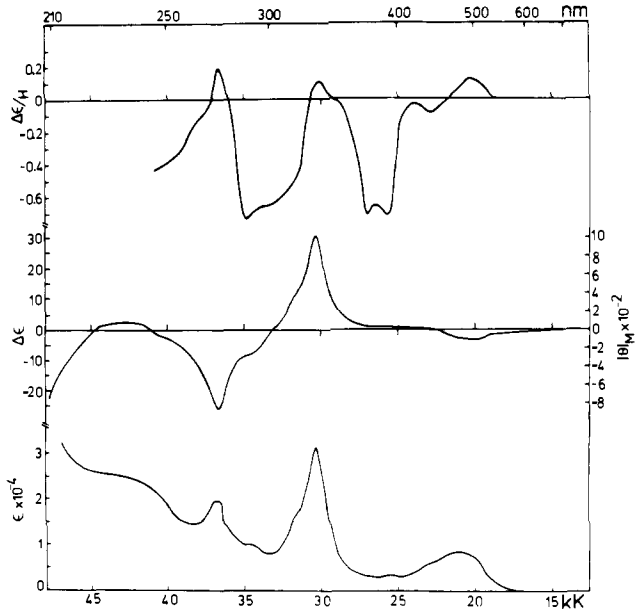

Figure 5. MCD (top), CD (middle), and optical (bottom) spectra of copper cobalamin in water at neutral pH and ambient temperature. The spectra were calibrated using ϵ_{490} = 8333 (ref 5b). Units are ϵ (L/(mol·cm)), $\Delta\epsilon/H$ (L/(mol·cm·T)), and $[\theta]_M$, the molar ellipicity (deg/(mol·cm^2)).

Optical, CD, and MCD Spectra. In Figure 5 are shown the optical, circular dichroism (CD), and magnetic circular dichroism (MCD) spectra of the copper corrins. In the CD spectrum, allowing for the position shifts due to the metal insertion, the signs of the CD bands are the same as seen in the metal-free cobinamide.[17] In comparison with cobalt cobalamins, each of the CD absorptions differs significantly in both sign and relative position with regard to their associated optical band.[18] The differences in the CD between the cobalt and metal-free corrins were attributed to the influence of the metal interactions through orbital mixing.[17]

Relative to the absorption spectrum, the MCD spectrum is dissimilar to those of both cobalt (II) and cobalt(III) cobinamides. And even though the complex contains a paramagnetic copper ion, the size of the MCD effect is a factor of about 30 smaller than that of the paramagnetic cobalt(II) complex and about the size of the diamagnetic cobalt(III) compound.[19] The above data strongly suggest that, since the spectroscopic transitions arise basically from the π–π^* transitions, the paramagnetic electron in the $d_{x^2-y^2}$ orbital does not interact in any major way with the π-electron system of the macrocycle. This is the same conclusion reached by Schreiner et al. for a porphyrin complex of copper.[20] This result also suggests that the copper resides in the plane of the macrocycle ring.

Thus, the copper corrin complex presents us with a molecule with its σ- and π-bonding effects naturally separated to a high order. (The two types of orbitals are of course mixed by spin–orbit coupling as seen in the shift in g values.) This natural separation allows us to describe the σ bonding in these tetrapyrrole macrocycles in a particularly simple way as will be shown below. The spectra and energies of the π orbitals have been discussed extensively for both the corrins[21] and the porphyrins.[22]

Discussion

Orbital Energy Level Analysis. Care must be taken in comparing copper porphyrins with the copper corrin. As mentioned above, the copper corrin in aqueous solutions and methanol

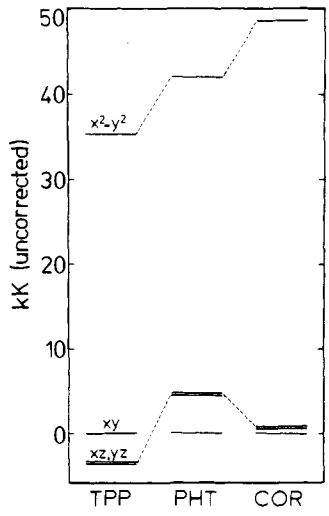

Figure 6. Energy levels of copper calculated from elementary perturbation theory (eq 2) from the EPR g values for tetraphenylporphyrin (TPP), phthalocyanine (PHT), and corrin (COR). No correction for an "orbital reduction factor" has been made. The d_{xy} orbital is *assumed* fixed at zero. This is not the same zero energy as seen in Figure 7.

exhibits no fundamental change in EPR spectra with the addition of high concentrations of coordinating ligands such as pyridine. This is no surprise since even the imidazole covalently attached to the macrocycle does not bind to the copper. On the other hand, addition of pyridine significantly changes the porphyrin EPR spectrum as it binds to the metal.

To clarify this point, ^{63}Cu was inserted into coproporphyrin I tetramethyl ester (the generous gift of Dr. Mike Turnbull). This is a porphyrin with four proprionic acid side chains: one on each pyrrole. The ester is soluble in nonpolar solvents, and the tetraacid in water, methanol, etc. Thus, the compound allows the same chromophore to be dissolved in both benzene and methanol while free of spurious inductive effects. Clear differences in the EPR spectra were seen indicating that even methanol may be binding at least weakly to the copper in the porphyrin. The difference must result from the diminished acidity of the copper in the corrin. Apparently a small shift of electron density onto the copper in the corrin, as reflected by the small increase in the hyperfine splitting, is sufficient to prevent further binding by nucleophilic species.

Given this difference, for comparison with the four-coordinate copper corrin, we choose copper tetraphenylporphyrin in the solid state, since its structure[23] indicates that there will be no axial ligation. The ^{63}CuTPP:ZnTPP has been accurately characterized by Hoffman,[13] and his ENDOR results for this porphyrin have been used for comparison with our data on the copper corrin. Also, only the g values of copper phthalocyanine are considered reliable enough to use.

In Figure 6 we show the energies of the optical transitions calculated from the g values using the equations for d^9 ions:

$$g_{\parallel} = g_e + 8\lambda/\Delta_1$$
$$g_{\perp} = g_e + 2\lambda/\Delta_2 \qquad (2)$$

where λ is the one-electron spin-orbit coupling constant (-830 cm^{-1}), g_e is the free-electron g value (2.0023), and Δ_1 and Δ_2 are the energy splittings between the $d_{x^2-y^2}$ orbital and the d_{xy} and $d_{xz,yz}$ orbitals, respectively. We have made no correction for the covalency using an "orbital reduction factor" or some function of molecular orbital coefficients since neither is clearly relatable to the complicated bonding.[24] In addition, we are mostly interested in the *relative* trends of the series porphyrin, phthalocyanine, and corrin, and any variation in "orbital reduction factor" through the series should be small and will not affect the following discussion. In general, any isotropic corrections will merely multiply the energy scale in the figure by some fraction less than 1. On the other hand, the possibility does exist that anisotropy in a reduction factor may raise the $d_{xz,yz}$ sets relative to the d_{xy} about equally over the series. Nevertheless, the relative levels between compounds should not change and, again, will not fundamentally affect any conclusions.

Table II. Metal-N Distances (in Å)

	Co(III)	Ni(II)	Cu(II)
corrin	1.904[a]	1.865[b]	(1.91)[g]
TPP	1.978[c]	1.928[d]	1.981[e]
	0.074	0.063	(0.07)
PHTH			1.934[f]

[a] K. Venkatesan, D. Dale, D. C. Hodgkin, C. E. Nockolds, F. H. Moore, and B. H. O'Connor, *Proc. R. Soc. London, Ser. A*, **323**, 455-487 (1971). [b] J. D. Dunitz and E. F. Meyer, Jr., *ibid.*, **288**, 324-330 (1965). [c] W. R. Scheidt, J. A. Cunningham, and J. L. Hoard, *J. Am. Chem. Soc.*, **95**, 8289-8294 (1973). [d] J. L. Hoard in "Porphyrins and Metalloporphyrins", K. M. Smith, Ed., Elsevier, Amsterdam, 1975, p 349. [e] E. B. Fleischer, C. K. Miller, and L. E. Webb, *J. Am. Chem. Soc.*, **86**, 2342-2347 (1964). [f] C. J. Brown, *J. Chem. Soc. A*, 2488 (1968). [g] Parentheses indicate an estimated value.

We have *arbitrarily* chosen the d_{xy} orbital in all three cases equal to zero as a reference energy. In effect, this says the in-plane p orbitals on the nitrogen ligands are involved in bonding with the two adjacent carbon atoms in the pyrrole rings: the metal-d_{xy} interaction energies are small and possibly the same for all three compounds. This assumption is also not crucial since we are more interested in the direction of the changes in the relative energies.

From Figure 6, two points are obvious. First, comparing the $d_{xz,yz}$ and the d_{xy} interactions, in the corrin and phthalocyanine the energies of these orbitals are inverted relative to the porphyrin. Since this must result from a back-bonding interaction from the filled d orbitals on the copper, the corrin is a worse π acceptor (better π donor) than the porphyrin. The change in magnitude of splitting energies with Cu-N distance (see Table II) is clearly not a simple function as seen by the relative energies for the phthalocyanine. Thus, beyond the simple analysis given immediately above, we do not wish to deal with this clearly complicated phenomenon.

The second point is that the result of the σ bonding on the energies appears quite simple with a monotonic increase of the energy of the $d_{x^2-y^2}$ orbital with a decreasing Cu-N distance (see Table II).

We can tentatively extend the semiquantitative analysis of the copper energy levels to the corrin containing cobalt: vitamin B_{12} and the B_{12} coenzymes. We use the ideas of the angular overlap model of bonding to advantage here to understand the differences in axial bonding between porphyrin and corrin. We assume approximate transferability of the energies between cobalt and copper. We find that for the square planar configuration ready to accept an axial ligand, the destabilization in energy of the $d_{x^2-y^2}$ orbital as a result of the σ bonding will be three times that of the d_{z^2}.[25] The change in the d_{z^2} arises from overlap of its taurus in the ligand plane. So, while the $d_{x^2-y^2}$ orbital in corrin will be on the order of 10 000 cm^{-1} higher than in the porphyrin, the d_{z^2} will be raised about 3000 cm^{-1} $\approx$ 0.4 eV. Ignoring solvent effects, this will result in a reduction of stability in axial bonding for the cobalt corrin vs. the cobalt porphyrin due to the d orbital's effects. Additionally, the raising of the $d_{xz,yz}$ orbitals (see Figure 6) further reinforces this reduction through the axial π bonding.

Hyperfine Coupling Analysis. We see from the data in Table I that the difference in the spin localization is relatively small between the porphyrin and corrin. From arguments made

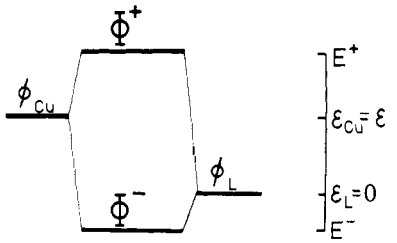

Figure 7. Diagram defining the terms of the general two-level molecular orbital scheme used to describe the σ bonding.

above from the MCD spectra, we found the paramagnetic electron is localized in the σ-bonding orbitals and that they are separated from the π-bonding orbitals. Since our measurements of the hyperfine coupling can be made relatively accurately, we can calculate the paramagnetic electron's distribution among the copper and its nitrogen ligands in a simple and direct manner. The following assumptions are needed. (1) The electron is localized on the copper and nitrogens only. (2) The nitrogen atoms are effectively equivalent. (3) The hybridization of the orbitals involved in the isotropic hyperfine splittings is constant. (4) The hyperfine interaction is proportional to the amount of paramagnetic electron "on" an atom in the molecule. The third assumption is reasonable, since within experimental error, the isotropic and anisotropic copper hyperfine splittings both show the same relative change.

In analogy with the transfer of liquid between tanks, any transfer of spin between the metal and ligand will cause a *relative* change in the isotropic hyperfine coupling that is *inverse* to the *total paramagnetic electron already present.* Thus, by replacing porphyrin by corrin, the relative changes in hyperfine splittings (see Table I) are:

$$\text{for copper, } (286 - 273 \text{ MHz})/273 = 13/273 = 0.04_7;$$

$$\text{for each nitrogen, } (47.6 - 46 \text{ MHz})/47.6 = 1.6/47.6 = 0.03_5$$

Each of the nitrogens contributes one-quarter of the change on copper, that is 0.012. The relative change is then $\delta_{Cu}/\delta_L = 0.012/0.035 = 0.3_4$, leading to an absolute electron spin density (subject to assumption 1) of $1/(1 + 0.34) = 0.7_4$ on the copper and $0.34/1.34 = 0.25$ on the four nitrogens, or 0.06 on each nitrogen. These are average values for both macrocycle ligands.

We now have the following information on the σ-bonding system of corrin and porphyrin. We have quantified the increase of spin density on the copper and a concomitant decrease on the nitrogens. From the data and the assumed localization of spin we have calculated approximate, absolute values of electron spin densities. Also, with an increase of spin density on the copper in a molecule, we find the energy of the orbital containing the unpaired electron rises.

We wish to fit this data in as general a manner as possible with a minimum number of variables: a simple two-level metal–ligand molecular orbital scheme is sufficient. Referring to Figure 7 for definitions, the wave functions are:

$$\Phi^+ = C_L^+\phi_L + C_{Cu}^+\phi_{Cu}$$
$$\Phi^- = C_L^-\phi_L + C_{Cu}^-\phi_{Cu} \qquad (3)$$

ϕ_L is probably an agglomeration of orbitals with the appropriate symmetry for binding having relatively closely spaced energy levels.[26] In that case, $\mathscr{E}_L$ will represent their center of energy.

We wish to solve the secular determinant:

$$\begin{vmatrix} \mathscr{E}_L - E & B - SE \\ B - SE & \mathscr{E}_{Cu} - E \end{vmatrix} = 0$$

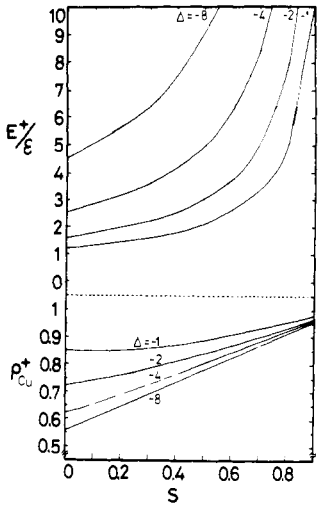

Figure 8. Plot of the values of the variables calculated from eq 4 and 6 with $\mathscr{E}_L = 0$.

where B is a generalized perturbation and S is the overlap integral, $\langle\phi_{Cu}|\phi_L\rangle$. The solutions of this equation are:

$$E^{\pm} = \frac{A - BS \pm \sqrt{D^2(1 - S^2) + (B - AS)^2}}{1 - S^2} \qquad (4)$$

where $\mathscr{E}_L = A + D$ and $\mathscr{E}_{Cu} = A - D$.

From the secular equation, we can determine the wave function coefficients for Φ^+ to be:

$$C_{Cu}^+ = [(M^+)^2 + 1]^{-1/2}$$
$$C_L^+ = M^+C_{Cu}^+ \qquad (5)$$

with $M^+ = (B - SE^+)/E^+$. The same equations hold for Φ^- with a change of superscript.

To compare with the experimentally determined spin densities, we calculate from eq 3:

$$\rho_{Cu}^+ = C_{Cu}^+\langle\phi_{Cu}|\Phi^+\rangle = C_{Cu}C_LS + C_{Cu}^2$$
$$\rho_L^+ = C_L^+\langle\phi_L|\Phi^+\rangle = C_L^2 + C_{Cu}C_LS$$

The paramagnetic electron is in the anti-bonding orbital, Φ^+, which in the limit becomes the $d_{x^2-y^2}$ copper orbital. Figure 8 shows some calculated curves of ρ_{Cu}^+ and E^+ vs. Δ and S. The plots use $\Delta = 2B/\mathscr{E}$ as a reduced variable. Here the ligand orbital energy $\mathscr{E}_L = 0$ arbitrarily, and we call $\mathscr{E}_{Cu} = \mathscr{E}$ (equivalent to letting $A = -D$ in eq 4).

We do not hope to fit the data exactly, especially since the value of $\mathscr{E}$ is not allowed to change. Its value will depend on the effective charges on the atoms in the molecule before "turning on" their interactions. These charges are difficult to guess or calculate since, first, the corrin ring is a monoanion and the porphyrin a dianion, and, second, we expect the π system to delocalize some unknown part of the charge.

We note again that quantitation of changes in the EPR spectra here is at the limit of our polycrystalline data. So we are satisfied to have (1) the trends in E^+ and ρ_{Cu}^+ between the corrin and porphyrin fit and (2) the electron-spin density approximately 70% on the copper and the remainder on the set of four nitrogens. We see that to have ρ_{Cu}^+ be between 0.65 and 0.75, Δ must be large, in the range -2 to -4; B is larger than $\mathscr{E}$.[27] From this analysis, no preferred values for S can be ascertained, although for d orbitals it is calculated to be small (<0.2).[21] Also, this analysis suggests that the increase in ρ_{Cu}^+ and E^+ resulting from exchanging corrin for porphyrin arises predominantly from an increase in S, the overlap, without a change in Δ.

Acknowledgments. It is a pleasure to thank Professor Jack Lewis for his constant encouragement. Also, we wish to thank Andrew Thomson, Roger Sealy, and Jim Hyde for obtaining experimental data and Malcolm Gerloch, Peter Boyd, and Guy Woolley for clarifying discussions on the theoretical aspects of the bonding.

References and Notes

(1) This work was carried out while the author was in receipt of postdoctoral fellowships from the National Institutes of Health, NATO, administered by the National Science Foundation, and the Science Research Council of Great Britain. Parts of the work were supported by grants from the SRC to Professor J. Lewis. The ESR Service Center, Milwaukee, is sponsored by the National Institutes of Health.
(2) (a) T. C. Stadtman, *Science*, **171**, 859–867 (1971). (b) R. Bonnett, *Chem. Rev.*, **63**, 573–604 (1963).
(3) E.g., R.-h. Yamada, S. Shimizu, and S. Fukui, *Biochemistry*, **7**, 1713–1719 (1968).
(4) B. Briat and C. Djerassi, *Bull. Soc. Chim. Fr.*, 135–146 (1969).
(5) (a) V. B. Koppenhagen and J. J. Pfiffner, *J. Biol. Chem.*, **24**, 5865–5873 (1970). (b) V. B. Koppenhagen and J. J. Pfiffner, *ibid.*, **246**, 3075–3077 (1971). (c) V. B. Koppenhagen, F. Wagner, and J. J. Pfiffner, *ibid.*, **248**, 7999–8002 (1973). (d) V. B. Koppenhagen, B. Elsenhans, F. Wagner, and J. J. Pfiffner, *ibid.*, **249**, 6532–6540 (1974).
(6) (a) J. I. Toohey, *Proc. Natl. Acad. Sci. U.S.A.*, **54**, 934–942 (1965). (b) J. I. Toohey, *Fed. Proc., Fed. Am. Soc. Exp. Biol.*, **25**, 1628–1632 (1965).
(7) V. Koppenhagen, E. Warmuth, and F. Wagner, *Symp. Tech. Mikrobiol. (Berlin)*, 323–328 (1973).
(8) D. J. Arnon, V. S. R. Das, and J. D. Anderson, *Microalgae Photosynthetic Bacteria*, 529–545 (1963).
(9) H. Vogelmann and F. Wagner, *J. Chromatogr.*, **76**, 359–379 (1973).
(10) B. S. Grainger and K. A. Rubinson, *J. Phys. E.*, 773–775 (1977).
(11) C. M. Guzy, J. B. Raynor, and M. C. R. Symons, *J. Chem. Soc. A*, 2299–2303 (1969).
(12) To our knowledge, the correct conversion of coordinates has not been simply stated in the literature and is shown here. Implicit is the assumption that $A_{xN} = A_{yN} = A_{\perp N}$, which is effectively the case for the porphyrin.[13] First, convert $A_{\perp N}$ and $A_{\parallel N}$ expressed in gauss either to cm^{-1} or MHz using the equations: $A_i(cm^{-1}) = 0.9348(g_i/g_e) \times 10^{-4} A_i(G)$ or $A_i(MHz) = 2.8025(g_i/g_e)A_i(G)$, respectively. In this step, both ^{63}Cu and ^{14}N hyperfine values are treated in the same manner, since each nucleus interacts independently with the unpaired electron. These hyperfine values are now effectively "corrected" to $g = g_e$ and are converted to the nitrogen coordinate system using eq 1a and 1b. Equation 1b arises from the averaging of the hyperfine interactions over all orientations of the macrocycle plane with most of the contribution arising from the orientations with four nitrogens equivalent being enhanced over those with the nitrogens equivalent in pairs. This is due to the number of EPR transitions arising from each. (We are indebted to a referee for clarifying this point.) Finally, all values of hyperfine energies should be expressed in energy units—preferably either MHz or cm^{-1}.
(13) T. G. Brown, J. L. Petersen, G. P. Lazos, J. R. Anderson, and B. M. Hoffman, *Inorg. Chem.*, **16**, 1563–1565 (1977).
(14) G. Feher, R. A. Isaacson, C. P. Scholes, and R. Nagel, *Ann. N.Y. Acad. Sci.*, **222**, 86–101 (1973).
(15) G. H. Rist and J. S. Hyde, *J. Chem. Phys.*, **52**, 4633–4643 (1970).
(16) L. Kevan and L. D. Kispert, "Electron Spin Double Resonance Spectroscopy", Wiley, New York, 1976, Section 4.6.
(17) A. J. Thomson, *J. Am. Chem. Soc.*, **91**, 2780–2785 (1969).
(18) (a) R. D. Fugate, C.-A. Chin, and P.-S. Song, *Biochim. Biophys. Acta*, **421**, 1–11 (1976). (b) R. A. Firth, H. A. O. Hill, J. M. Pratt, R. J. P. Williams, and W. R. Jackson, *Biochemistry*, **6**, 2178–2188 (1967). (c) K. Sato, S. Shimizu, and S. Fukui, *Biochem. Biophys. Res. Commun.*, **39**, 170–174 (1970).
(19) B. Briat and C. Djerassi, *Nature (London)*, **217**, 918–922 (1968).
(20) A. F. Schreiner, J. D. Gunter, D. J. Hamm, I. D. Jones, and R. C. White, *Inorg. Chim. Acta*, **26**, 151–155 (1978).
(21) (a) P. Day, *Theor. Chim. Acta*, **7**, 328–341 (1967). (b) P. O'D. Offenhartz, B. H. Offenhartz, and M. M. Fung, *J. Am. Chem. Soc.*, **92**, 2966–2973 (1970).
(22) (a) M. Gouterman, *J. Mol. Spectrosc.*, **6**, 138–163 (1961). (b) M. Zerner and M. Gouterman, *Theor. Chim. Acta*, **4**, 44–63 (1966).
(23) E. B. Fleischer, C. K. Miller, and L. E. Webb, *J. Am. Chem. Soc.*, **86**, 2342–2347 (1964).
(24) M. Gerloch, J. Harding, and R. G. Woolley, *Proc. R. Soc. London, Ser. A*, in press.
(25) M. Gerloch and R. C. Slade, "Ligand Field Parameters", Cambridge University Press, Cambridge, 1973, p 177.
(26) P. J. Derrick, L. Ashbrink, O. Edqvist, B.-O. Jonsson, and E. Lindholm, *Int. J. Mass Spectrom. Ion Phys.*, **6**, 191–202 (1971).
(27) We choose S to be positive, and since B/S must be a negative quantity, B is negative. Since in general δ is considered positive, we require that $\Delta < 0$.

Communications to the Editor

Synthesis, Structure, and Stereochemical Implications of the $[Pt_{19}(CO)_{12}(\mu_2\text{-}CO)_{10}]^{4-}$ Tetraanion: A Bicapped Triple-Decker All-Metal Sandwich of Idealized Fivefold (D_{5h}) Geometry

Sir:

We report here the preparation and structure of a 19-metal-atom cluster, the $[Pt_{19}(CO)_{22}]^{4-}$ tetraanion. This remarkable polynuclear metal species was prepared by Ceriotti, Longoni, and Chini. The metal framework together with the 10 bridging and 2 axial carbonyl ligands were established by Washecheck and Dahl and later substantiated by Manassero and Sansoni from X-ray structural determinations of the $[n\text{-}Bu_4N]^+$ salt. The complete structure was determined for the $[Ph_4P]^+$ salt by Washecheck and Dahl. The salient structural feature is that the entire platinum carbonyl cluster contains a pseudofivefold principal axis, which is without precedent in discrete transition metal clusters but which has been found for small metallic crystallites on heterogeneous surfaces. In addition, this complex provides the first example of a metal carbonyl cluster with (1) 19 homonuclear metal atoms—the largest discrete metal aggregate reported to date; (2) two completely encapsulated metal atoms; and (3) a CO-to-(total metal) ratio of 22:19 = 1.16, which is considerably less than the previously known lowest value of ~1.7 for other metal carbonyl species. The CO-to-(surface metal) ratio of 22:17 = 1.29 is closest to the situation observed for the chemisorption of carbon monoxide either on platinum single crystal surfaces or on small platinum particles of the type used in supported metal catalysts, for which the maximum CO-to-(surface metal) ratio is ~0.75.[1] These characteristics indicate that its as yet unknown physicochemical properties may provide a better model for the properties of small metal aggregates[2] than those of any other previously reported discrete metal cluster.

This work is an outgrowth of systematic studies by Chini, Longoni, and co-workers[3] who have prepared a large number of nickel and platinum carbonyl cluster anions. Those isolated and structurally characterized include the $[M_3(CO)_3(\mu_2\text{-}CO)_3]_n^{2-}$ dianions (n = 2, 3 for M = Ni; n = 2–5 for M = Pt),[3a-d,f] the $[Ni_5(CO)_9(\mu_2\text{-}CO)_3]^{2-}$ dianion,[3e,f] and the $[Ni_{12}(CO)_{21}H_{4-n}]^{n-}$ anions (n = 2–4).[3i,j]

In the synthesis of the $[Pt_3(CO)_3(\mu_2\text{-}CO)_3]_n^{2-}$ oligomers,[3a,f] brown side products were obtained. Refluxing of the triangular platinum clusters in acetonitrile solution was found to produce these brown ionic compounds in good yields. In addition, other brown compounds were detected from infrared carbonyl spectral measurements of the reactions of these brown compounds with either acid or oxidizing agents. The isolation of the $[Pt_{19}(CO)_{22}]^{4-}$ tetraanion in crystalline form for structural analysis has required extensive work involving the use of nine different cations. In this communication the results of three X-ray diffraction determinations of this Pt-19 tetraanion are presented.

This compound was obtained in ~50% yield by a heating of the appropriate salt of the $[Pt_3(CO)_3(\mu_2\text{-}CO)_3]_3^{2-}$ dianion in refluxing acetonitrile. Anal. on the vacuum-dried product. Found: NBu_4, 17.37 (calcd, 18.3); Pt, 74.02 (calcd, 70.00);

0002-7863/79/1501-6110$01.00/0